JOURNAL OF GUIDANCE, CONTROL, AND DYNAMICS
Vol. 20, No. 5, September–October 1997

Development of Structural Uncertainty Models

Mark E. Campbell* and Edward F. Crawley†
Massachusetts Institute of Technology, Cambridge, Massachusetts 02139

The development and utilization of an uncertainty model for structures that undergo a change in operational environment is presented. The motivating application is the development of an on-orbit (0-*g*) uncertainty model for structural control based solely on ground (1-*g*) modeling and experimentation, although other applications can be used. A parametric uncertainty model (mean errors and bounds on modal parameters) is developed for a nominal environment and then localized to specific degrees of freedom (mass and stiffness uncertainties) using a first-order sensitivity method. The nominal mass and stiffness uncertainties are then projected into a modified environment to create an analogous, modified uncertainty model. The middeck active control experiment is introduced to verify the prediction of a space-based uncertainty model.

I. Introduction

MANY engineering applications require prediction of system dynamics and uncertainties based solely on modeling and testing in an environment that is different than its eventual use: modeling and testing of wings and rotorcraft in a wind tunnel prior to flight, redesign of a structure based on a nominal design, and modeling and testing of space structures on the ground. In addition, the required accuracy of these models is usually very high. For example, a high-precision space telescope must utilize a high-authority control design, which in turn requires a very accurate model of the dynamics to ensure stability and performance. The objective of this work is to develop an accurate description of a structural system (model and uncertainties) in both a nominal and modified environment, based solely on modeling and experimentation in the nominal environment.

Two common approaches exist for model development: analytical models based on geometric and material properties and system identification based on measured input–output data. Although a finite element model (FEM) is a physical description of the system, it is usually large and requires a model update step to be relatively accurate. A measurement model is a single model fit to a set of input–output data and is more accurate than the FEM. The measurement model, however, gives a nonphysical input–output description of the system, introducing unwanted effects such as multiple modes. Whereas both methodologies have their benefits and drawbacks, both also rely on a single set of data (for updating or fitting) used to represent the structure in a linear manner. The actual parameters of all structural systems, however, usually vary due to effects such as joint pretension, damping, sensor noise, and nonlinearities. Therefore, the most accurate and useful description of a structural system is a linear model and model of uncertainties.

Figure 1 shows the process for the development of an uncertainty model for a structural system in both a nominal and a modified environment. An FEM is developed and updated using open-loop data to obtain good accuracy, whereas additional dynamics for sensors, actuators, time delays, etc., are appended to create an input–output model. Using a large number of identification experiments, a set of measurement models is found. By comparing measurement models and the FEM-based input–output model, a nominal uncertainty model consisting of mean errors and bounds on critical parameters is developed. Finally, using the nominal and modified FEMs and the nominal uncertainty model, a modified uncertainty model can be predicted. It is noted that the FEM is used as the final linear model description because it is physical in nature and is linear, and the derivation of a model of modal uncertainties is easier because there are no multiple modes.

The development of an accurate modified uncertainty model is a complex blending of analytical modeling and updating, identification, probability analysis, and finite element error localization. Error localization techniques[1–3] attempt to localize errors to specific degrees of freedom using measured frequencies and mode shapes and an FEM. Sidhu and Ewins[4] developed the most well-known error localization method, called the error matrix method,[4,5] where a system is first reduced to the measured degrees of freedom, and errors in the flexibility matrix are identified and then inverted to find the measured stiffness errors. The sensitivity method[6,7] expresses mass and stiffness error matrices as a function of physical parameters and calculates first-order sensitivities. The force balance method[8] examines the system for large eigensystem residues using (expanded) experimental mode shapes and frequencies, thus indicating errors at specific degrees of freedom. There are also frequency-domain methods that build an error matrix as a function of frequency.[9,10]

One of the most thorough examinations of the repeatability of ground and space hardware is the Middeck 0-*g* Dynamics Experiment (MODE).[11] On the ground and in space, variations in modal parameters were examined as functions of disturbance force amplitude, joint preload, reassembly, shipset (different hardware), and suspension. Collins et al.[12] assume statistical properties for modeling parameters in order to iteratively localize uncertainties. This is very similar to the sensitivity method, except the variances are chosen to reflect the user's confidence in the parameter estimate. Hasselman et al.[13,14] group together generically similar structures into three databases, an example of which is research models of large (truss type) space structures. The databases can then be used to create a probability model of a space structure, consisting of a mean model and distribution of modal errors.

The approach of this paper is as follows. First, an assessment of structural modeling uncertainties is given to understand what types of errors must be captured in the uncertainty model. Then, the development of the nominal uncertainty model is presented, followed by the sensitivity-method-based projection process to predict the modified uncertainty model. Finally, the middeck active control experiment, a Shuttle flight experiment, which flew on STS-67 in March 1995, is introduced to experimentally verify the prediction of a modified uncertainty model using two distinct examples.

II. Assessment of Modeling Uncertainties

A thorough understanding of all possible modeling uncertainties in a structural system is very important to both the development of a nominal uncertainty model and the prediction of a modified uncertainty model. All uncertainties can be divided into the general groups of linear and nonlinear. Within these groups, five subgroups can be defined: physical, modeling, coupling, testing, and nonlinearities. Table 1 gives a summary of these uncertainties, along with their type (mean and/or variance) and capturability, or the ability to

Received March 18, 1996; revision received May 16, 1997; accepted for publication May 16, 1997.

*Research Associate, Space Engineering Research Center, Room 37-375, 77 Massachusetts Avenue. Member AIAA.

†Professor of Aeronautics and Astronautics and MacVicar Faculty Fellow, Director, Space Engineering Research Center. Fellow AIAA.

Table 1 Types of structural modeling uncertainties listed as mean and/or variance in type and ease or difficulty to capture them in a physical uncertainty model

			Uncertainty		Capturable	
Group	Subgroup	Type	Mean	Variance	Easy	Difficult
Linear	Physical modeling	Material	√		√	
		Geometric	√		√	
	Modeling method	Discretization	√			√
		Incorrect element physics	√			√
		Unmodeled dynamics	√			√
	Coupling	Boundary conditions	√	√	√	
		Joints/attachments	√	√	√	
		Actuator/sensor dynamics	√		√	
		Time delays	√		√	
		Gravity	√	√	√	
		Aerodynamic	√	√		√
		Controller	√	√	√	
	Testing procedure	Sensor/process noise	√	√	√	
		Sensor bias	√	√		√
Nonlinear	Weak		√	√	√	
	Strong		√	√		√

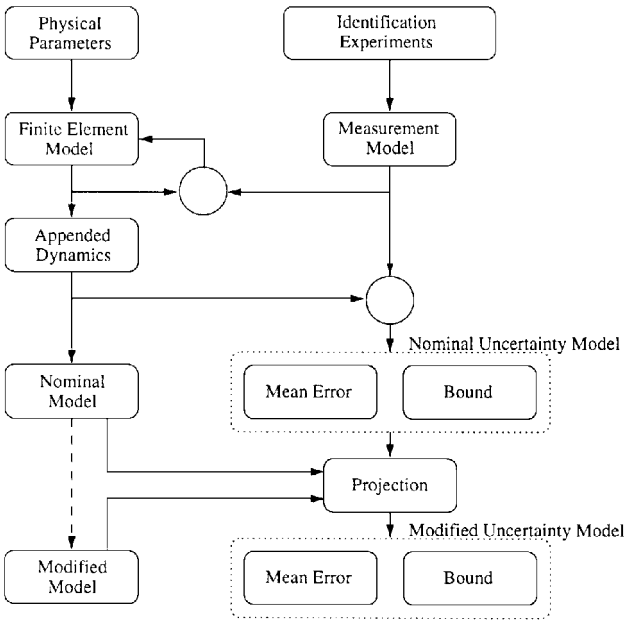

Fig. 1 Development process for system and uncertainty models.

localize an uncertainty to a physical mass/stiffness uncertainty as either easy or difficult.

Physical modeling uncertainties are those where the physics of the system has been captured correctly, but a number of the modeling parameters are in error. These uncertainties, which are traditionally treated with updating techniques, can be divided into two smaller groups: material uncertainties, such as the modulus of elasticity, density, etc., and geometric uncertainties, such as area and inertia (or their primitives such as radius and width), etc. These uncertainties are also the easiest to be captured because they are usually constant (mean error uncertainty). Modeling uncertainties, on the other hand, are those errors in which the physics of the hardware has not been represented correctly, including discretization issues, selection of correct element types, or unmodeled boundary conditions. Because the physics has not been captured correctly, these uncertainties are usually quite difficult to localize.

Coupling dynamics are those dynamics that are usually not modeled with finite elements and must be coupled in after the solution is found. The physics of the coupling dynamics is assumed to be modeled correctly, and only the parameters of the coupling dynamics are in error. (If the physics is not modeled correctly, the uncertainties are in the modeling method subgroup.) Coupling dynamics can include boundary conditions, joints/attachments, actuator and sensor dynamics, time delays, and many other types, which are not detailed here. These dynamics can easily lead to mean or even variance errors. For instance, if a structure is on a suspension system, every test may have slightly different boundary conditions. There are also other coupling dynamics that are termed external and are a function of the system environment. This includes gravity effects and aerodynamic effects and applying a closed-loop controller.

The testing procedure can also introduce uncertainties into the development of a system model. Issues, such as noise, bias, and amplifier gains of different sensors, along with the actual parameter estimation method can all impede accurate measurements of the system. A strain gauge, for example, is a sensor that is very dependent on the attachment to the system. For small noise and bias uncertainties, these can be represented using the uncertainty model. Large bias errors, however, cannot be represented as a linear physical change to the system.

Nonlinearities act on every system in some form: material properties, stiction, dead band stiffness in joints, and changing boundary conditions such as loss of tension in a cabled suspension system. Strong nonlinearities only degrade the localization process and usually require a nonlinear model, in addition to the FEM. If they are weak, or can be made weak by the addition of another component such as a closed-loop controller, these types of nonlinearities can be represented using variance uncertainties.

III. Uncertainty Model Development

The uncertainties described in the preceding section demonstrate that, when comparing a linear model with a structural system, both mean and variance errors exist. It is proposed to describe these errors using a stochastic uncertainty model, made up of a linear mean and bound (variance) on each of the parameters.

A. Problem Formulation

The nominal system dynamics can be described using an FEM:

$$M_N \ddot{\boldsymbol{q}}_N + C_N \dot{\boldsymbol{q}}_N + K_N \boldsymbol{q}_N = 0 \tag{1}$$

where $M_N \in \mathbb{R}^{n_N \times n_N}$ and $K_N \in \mathbb{R}^{n_N \times n_N}$ are the mass and stiffness matrices, respectively, and $\boldsymbol{q}_N$ is a vector of n_N physical degrees of freedom. Assuming proportional damping, an n_N-degree-of-freedom, linear structural generalized eigenvalue problem can be solved,

$$-M_N \Phi_N \Lambda_N + K_N \Phi_N = 0 \tag{2}$$

where $\Lambda_N \in \mathbb{R}^{n_N \times n_N}$ and $\Phi_N \in \mathbb{R}^{n_N \times n_N}$ are the eigenvalues and eigenvectors given by

$$\Phi_N = [\phi_{N1} \quad \ldots \quad \phi_{Nn_N}], \qquad \Lambda_N = \operatorname{diag}[\lambda_{N1} \quad \ldots \quad \lambda_{Nn_N}] \tag{3}$$

In addition, the eigenvectors are mass normalized, or

$$\Phi_N^T M_N \Phi_N = I, \qquad \Phi_N^T K_N \Phi_N = \Lambda_N \tag{4}$$

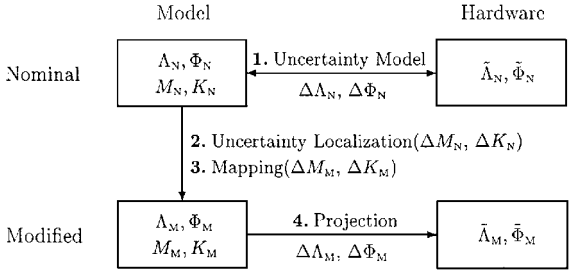

Fig. 2 Steps for the development of a modified uncertainty model.

The FEM is assumed to be an accurate representation of the hardware, such that the mean error and variance uncertainties can then be defined using a first-order perturbation to the nominal system, or

$$\begin{aligned} \tilde{M}_N &= M_N + \Delta M_N, & \tilde{K}_N &= K_N + \Delta K_N \\ \tilde{\Lambda}_N &= \Lambda_N + \Delta\Lambda_N, & \tilde{\Phi}_N &= \Phi_N + \Delta\Phi_N \end{aligned} \tag{5}$$

where the tilde refers to the linear model description of the hardware, i.e., data.

Assuming the nominal eigenvectors Φ_N are a sufficient set of basis vectors describing the hardware dynamics, changes in the eigenvectors, $\Delta\Phi_N$, can be written as a linear combination of the original eigenvectors,

$$\Delta\Phi_N = \Phi_N \Psi_N \tag{6}$$

It is assumed that all n_N eigenvalues and eigenvectors of the model are available. This assumption can be easily relaxed, although higher frequency eigenvectors create a sufficient basis for representing the eigenvalue perturbations, even though they might not be accurate. An analogous formulation of these equations can be developed for the modified system.

Figure 2 shows the approach for the uncertainty localization and projection process, given in four steps. 1) Given an FEM and data sets for the nominal system, an uncertainty model is developed, in the form of mean and covariance uncertainties of the eigenvalues and eigenvectors between the model and hardware. 2) These uncertainties are localized to specific physical degrees of freedom of the FEM, in the form of mean error and covariance uncertainties of the physical mass and stiffness matrices. 3) A mapping of degrees of freedom between the nominal and modified systems is used to create the mass and stiffness uncertainties of the modified system. 4) The modified FEM is used to project the mapped mass and stiffness uncertainties and predict the uncertainty model for the modified system in the form of mean and covariance uncertainties of the eigenvalues and eigenvectors. Each of these steps is examined in the following sections.

B. Step 1: Development of Nominal Uncertainty Model

The first step in this compilation of methods is the development of the nominal uncertainty model. A set of tests is needed to accurately measure each of the uncertainties itemized in Table 1. This can be done by varying test parameters such as using different actuators, sensors, disassembly/reassembly, time between tests, disturbance levels, and adding a nonstructural change such as a servo system. By testing each of these parameters, a large database of the nominal system response is created, thus measuring each of the uncertainties.

An identification/parameter estimation method is then used to find parameter estimates for the measured frequencies (eigenvalues) and eigenvectors of the system. This technique must parameterize the FEM and component models (sensor, actuator, time delays, etc.) separately and must allow easy extraction and combination of measured modal parameters. Once the parameters are identified, the nominal uncertainty model is created by calculating mean and covariance errors of critical parameters of the system. For the FEM, this is given as

$$E\begin{bmatrix} \text{vec}\{\Delta\lambda_{Ni}\} \\ \text{vec}\Delta\phi_{Ni} \end{bmatrix}, \qquad \text{cov}\begin{bmatrix} \text{vec}\{\Delta\lambda_{Ni}\} \\ \text{vec}\Delta\phi_{Ni} \end{bmatrix} \tag{7}$$

A complete explanation of this procedure is given in Ref. 15.

C. Step 2: Uncertainty Localization

With the nominal uncertainty model, the next step is to localize the FEM uncertainties to specific degrees of freedom. A first-order sensitivity method whose roots can be traced back three decades[6,12] is used. The method described here, however, develops a complete uncertainty localization strategy that not only uses first-order sensitivities, but also addresses problems such as systematically choosing update parameters and handling an insufficient number of modal measurements. In addition, the technique is adapted for the localization of variance uncertainties, as well as mean errors.

Enforcing the structural eigenvalue problem for the true dynamics of the nominal hardware

$$-\tilde{M}_N \tilde{\phi}_{Ni} \tilde{\lambda}_{Ni} + \tilde{K}_N \tilde{\phi}_{Ni} = 0 \tag{8}$$

by substituting Eqs. (5) and (6) into Eq. (8) and premultiplying by ϕ_{Ni}^T and ϕ_{Nj}^T yield

$$\Delta\lambda_{Ni} = \phi_{Ni}^T [\Delta K_N - \lambda_{Ni} \Delta M_N] \phi_{Ni} \tag{9}$$

$$[\lambda_{Ni} - \lambda_{Nj}] \psi_{Nji} = \phi_{Nj}^T [\Delta K_N - \lambda_{Nj} \Delta M_N] \phi_{Ni} \tag{10}$$

The mass and stiffness perturbations are assumed to be in the form

$$\Delta K_N = \sum_{j=1}^{k_N} \alpha_j K_j, \qquad \Delta M_N = \sum_{j=1}^{m_N} \beta_j M_j \tag{11}$$

where K_j and M_j are macroelements, α_j and β_j are scale factors that represent the relative size of each macroelement, and k_N and m_N are the total number of macroelements for the nominal system. A discussion of these macroelements is given subsequently. Substituting Eq. (11) into Eqs. (9) and (10) and rearranging, the eigenvalue and eigenvector errors are

$$\Delta\lambda_{Ni} = \sum_{j=1}^{k_N} \left[\phi_{Ni}^T K_j \phi_{Ni}\right] \alpha_j - \lambda_{Ni} \sum_{j=1}^{m_N} \left[\phi_{Ni}^T M_j \phi_{Ni}\right] \beta_j \tag{12}$$

$$\Delta\phi_{Ni} = \sum_{j=1}^{k_N} \left[\sum_{\substack{k=1 \\ k \neq i}}^{n_N} \frac{\phi_{Ni}^T K_j \phi_{Nk}}{\lambda_{Nk} - \lambda_{Ni}} \phi_{Nk} \right] \alpha_j - \sum_{j=1}^{m_N} \left[\sum_{\substack{k=1 \\ k \neq i}}^{n_N} \lambda_{Nk} \frac{\phi_{Ni}^T M_j \phi_{Nk}}{\lambda_{Nk} - \lambda_{Ni}} \phi_{Nk} - \frac{\phi_{Ni}^T M_j \phi_{Ni}}{2} \phi_{Ni} \right] \beta_j \tag{13}$$

These equations are linear in terms of the macroelemental scale factors α_j and β_j. Therefore, all of the measured errors can be written in the form

$$\begin{bmatrix} \text{vec}\{\Delta\lambda_{Ni}\} \\ \text{vec}\Delta\phi_{Ni} \end{bmatrix} = S_N \begin{bmatrix} \boldsymbol{\alpha}_N \\ \boldsymbol{\beta}_N \end{bmatrix} \tag{14}$$

where S_N is a sensitivity matrix.

A weighted pseudoinverse is used to calculate the macroelemental scale factors

$$\begin{bmatrix} \boldsymbol{\alpha}_N \\ \boldsymbol{\beta}_N \end{bmatrix} = [W_N S_N]^+ W_N \begin{bmatrix} \text{vec}\{\Delta\lambda_{Ni}\} \\ \text{vec}\Delta\phi_{Ni} \end{bmatrix} \tag{15}$$

where the plus superscript refers to the pseudoinverse and W_N is a diagonal weighting matrix

$$W_N = \text{diag}\left[\frac{c_{\lambda Ni}}{\|\lambda_{Ni}\|}, \frac{c_{\phi Nij}}{\|\phi_{Nij}\|} \right]$$

and $c_{(\,)}$ are relative confidence factors. For this case, the nominal parameter bounds give a measure of confidence in the estimate, such that a large bound indicates an estimate that varies widely

and might not be accurate. Therefore, the confidence factors are inversely proportional to the bounds:

$$c_{\lambda Ni} = \frac{\|\lambda_{Ni}\|}{\widehat{\lambda_{Ni}}}, \qquad c_{\phi Ni} = \frac{\|\phi_{Nij}\|}{\widehat{\phi_{Nij}}} \tag{16}$$

Because the macroelemental scale factors are linear in terms of the measured nominal uncertainty model, the expected value and covariance can easily be calculated:

$$E\begin{bmatrix}\alpha_N \\ \beta_N\end{bmatrix} = \left[[W_N S_N]^+ W_N\right] E\begin{bmatrix}\text{vec}\{\Delta\lambda_{Ni}\} \\ \text{vec}\Delta\phi_{Ni}\end{bmatrix} \tag{17}$$

$$\text{cov}\begin{bmatrix}\alpha_N \\ \beta_N\end{bmatrix} = \left[[W_N S_N]^+ W_N\right] \text{cov}\begin{bmatrix}\text{vec}\{\Delta\lambda_{Ni}\} \\ \text{vec}\Delta\phi_{Ni}\end{bmatrix} \left[[W_N S_N]^+ W_N\right]^T \tag{18}$$

D. Step 3: Mapping

The physical mass and stiffness uncertainties correspond to particular degrees of freedom; therefore, they can then be mapped to the modified system. For instance, suppose there is a truss structure with a plate that has a 5% mass error. If the plate is also in the modified structure, the mass error of the corresponding degree(s) of freedom is also 5%. Under this assumption, a mapping of degrees of freedom is created T_{MN}, or

$$q_M = T_{MN} q_N \tag{19}$$

In addition, because a number of macroelements only exist in the nominal system, such as the modeling of gravity effects in 1 g, the scale factors can be mapped as well:

$$\alpha_M = T_\alpha \alpha_N, \qquad \beta_M = T_\beta \beta_N \tag{20}$$

It follows that the mass and stiffness errors for the modified system are given by

$$\Delta K_M = \sum_{j=1}^{k_M} \alpha_j T_{MN} K_j T_{MN}^T, \qquad \Delta M_M = \sum_{j=1}^{m_M} \beta_j T_{MN} M_j T_{MN}^T \tag{21}$$

E. Step 4: Uncertainty Projection

The next step is to find the modified eigenvalue and eigenvector uncertainties in terms of the mass and stiffness uncertainties. An analogous derivation of the sensitivity equation, given in Eqs. (12–14) for the nominal system, can be developed for the modified system using the macroelements in Eq. (21):

$$\begin{bmatrix}\text{vec}\{\Delta\lambda_{Mi}\} \\ \text{vec}\Delta\phi_{Mi}\end{bmatrix} = S_M \begin{bmatrix}\alpha_M \\ \beta_M\end{bmatrix} \tag{22}$$

The expected mean and covariance are then easily calculated in terms of the measured uncertainties of the nominal system:

$$E\begin{bmatrix}\text{vec}\{\Delta\lambda_{Mi}\} \\ \text{vec}\Delta\phi_{Mi}\end{bmatrix} = P_{MN} E\begin{bmatrix}\text{vec}\{\Delta\lambda_{Ni}\} \\ \text{vec}\Delta\phi_{Ni}\end{bmatrix} \tag{23}$$

$$\text{cov}\begin{bmatrix}\text{vec}\{\Delta\lambda_{Mi}\} \\ \text{vec}\Delta\phi_{Mi}\end{bmatrix} = P_{MN} \text{cov}\begin{bmatrix}\text{vec}\{\Delta\lambda_{Ni}\} \\ \text{vec}\Delta\phi_{Ni}\end{bmatrix} P_{MN}^T \tag{24}$$

where

$$P_{MN} = S_M \begin{bmatrix}T_\alpha & 0 \\ 0 & T_\beta\end{bmatrix} \left[[W_N S_N]^+ W_N\right]$$

The mean errors and bounds for the critical parameters, i.e., uncertainty model, of the modified system can then be computed. The eigenvector mean errors ( ) and bounds ( ) are computed directly:

$$\overline{\Delta\phi}_{Mij} = E[\Delta\phi_{Mij}], \qquad \widehat{\Delta\phi}_{Mij} = 3 \cdot \sqrt{\text{var}[\Delta\phi_{Mij}]} \tag{25}$$

where var [ ] denotes the variance, or the diagonal of the covariance matrix. Note that the scaled standard deviation allows the user to adjust the conservatism of the bounds. Whereas the eigenvalue uncertainties can be found similarly, more meaningful uncertainties are in frequencies. Assuming the eigenvalue error is small compared to the eigenvalue, a first-order Taylor expansion can be used to calculate the mean errors and bounds on the frequencies

$$\overline{\Delta f}_{Mi} = \frac{E[\Delta\lambda_{Mi}]}{2f_M}, \qquad \widehat{\Delta f}_{Mi} = \frac{3 \cdot \sqrt{\text{var}[\Delta\lambda_{Mi}]}}{2f_{Mi}} \tag{26}$$

Uncertainties in coupling dynamics are usually identical in the nominal and modified environments. Damping uncertainties are usually quite difficult to project. Therefore, the modified damping uncertainties are usually chosen as highly scaled versions of the nominal damping bounds, thus being very conservative.

IV. Practical Implementation

Many times, methods are developed that work well for simple problems, but practical application of such methods is severely lacking. This section describes development of nominal and modified uncertainty models in a practical experiment, specifically addressing issues such as sensors, macroelements, practical algorithm, and accuracy of the uncertainty model.

A. Number of Sensors

In most practical applications, measurement of all degrees of freedom is not possible. Many error localization methods, however, require measurement of all degrees of freedom, reduction of the original system, or expansion of experimental mode shapes. Reduction of the original system leads to errors and error locations that are suspect.[5] There is no general correlation between the actual mode shape and the accuracy of the expanded mode shape.[16] The sensitivity method is one of the only methods that does not reduce or expand and that can use a subset of system measurements. In this work, the nominal uncertainty model is based on incomplete information: the number of measured frequencies is less than (or equal to) the number of FEM modes ($\tilde{n}_N \leq n_N$); the number of distinct actuators and sensors (measured mode shapes) is less than (or equal to) the number of FEM degrees of freedom ($r_N \leq n_N$).

B. Number of Macroelements

The localization of the nominal uncertainty model utilizes a pseudoinverse [as shown in Eq. (15)]. Although the weighting in the pseudoinverse is important, ensuring that Eq. (14) is overdetermined (more knowns than unknowns) is the primary factor in determining the accuracy of the pseudoinverse. The pseudoinverse of an overdetermined system is a classical least squares problem where a weighted quadratic error e_N,

$$e_N = E\begin{bmatrix}\text{vec}\{\Delta\lambda_{Ni}\} \\ \text{vec}\Delta\phi_{Ni}\end{bmatrix} - S_N E\begin{bmatrix}\alpha_N \\ \beta_N\end{bmatrix} \tag{27}$$

is minimized. For the underdetermined case, other constraints must be added to the problem because there are more unknowns than knowns. In this work, Eq. (14) is overdetermined if the number of macroelements is less than or equal to the number of measured errors, or

$$k_N + m_N \leq (r_N + 1) \cdot \tilde{n}_N \tag{28}$$

C. Types of Macroelements

Macroelements are user-defined matrices that attempt to span the space of all possible modeling errors. Therefore, many types of macroelements exist. Factors that influence the choices include: the number and location of the measurements, the number and type of modes, the types of uncertainties that may exist, and the size of the FEM. Because the practical case of requiring the number of macroelements is less than or equal to the number of measured errors is considered [Eq. (28)], three different types of macroelements are defined: subelements, elements, and groups of elements.

Subelement-based macroelements are those errors that lie within the physical parameters of the particular finite element, such as modulus of elasticity, density, and even gravity effects.[17] Errors in most coupling dynamics (except for gravity effects) are not

localized, but must be parameterized and estimated in the identification procedure.[15] Element-based macroelements are those errors that lie in different finite elements. A single macroelement can be formed that is the summation of all subelement errors corresponding to a finite element. This macroelement can then be used to localize errors to that element, even if the subelement errors are distinct.

Macroelements as groups of elements are those errors that lie in an area of the structure. Because a fine FEM mesh is required to eliminate discretization errors, all degrees of freedom are usually not experimentally measured. Therefore, it is useful to group finite element errors into one macroelement. The simplest grouping procedure is using insight from the modeling process. For instance, if an element is split into two equivalent elements to obtain a finer mesh, errors in these two finite elements can be grouped together into one macroelement for localization. A second method for grouping can also be used, which is a function of the experimental measurements. If a large area of the structure does not contain actuators or sensors, it is usually difficult to localize errors to these degrees of freedom. Taking a term from the control systems community, the element errors may be unobservable. Mathematically, these unobservable element errors manifest themselves as singularities in the sensitivity matrix. Therefore, macroelements (as well as sensor/actuator placement) can be developed such that the sensitivity matrix in Eq. (14) is full rank and well conditioned.

D. Practical Algorithm

The most accurate error localization utilizes subelement macroelements. Because of this, and with the constraint that the number of macroelements is less than the number of measured uncertainties [Eq. (28)], a special three-step procedure is used: 1) localize with macroelements: groups of elements, reduce number of macroelements; 2) localize with macroelements: elements, reduce number of macroelements; and 3) localize with macroelements: subelements, reduce number of macroelements.

The uncertainties are first localized to areas of the structure, using macroelements based on groups of elements. The number of macroelements is reduced by throwing out those macroelements that do not contain large modeling errors. This reduction is described subsequently. The remaining macroelements are then divided to create element-based macroelements. A similar procedure is used in steps 2 and 3, resulting in localized errors within each finite element parameter such as modulus of elasticity and density. Note that the strategy could start with step 2 or 3, depending on the number of measured errors.

The reduction is accomplished by examining the quadratic least squares cost of the pseudoinverse,

$$J = \boldsymbol{e}_N^T W_N^2 \boldsymbol{e}_N \tag{29}$$

where e_N is the error in Eq. (27) and W_N is the weighting matrix in Eq. (15). Figure 3 shows a sample plot of the normalized cost as a function of the number of macroelements used (12 total). At each step, each macroelement is eliminated, and the cost is evaluated. The macroelement that reduces the cost the least is then eliminated. This procedure is repeated until only one macroelement is left. This reduction procedure gives a rough ordering of the importance of the macroelements to the pseudoinverse and, therefore, a minimum number.

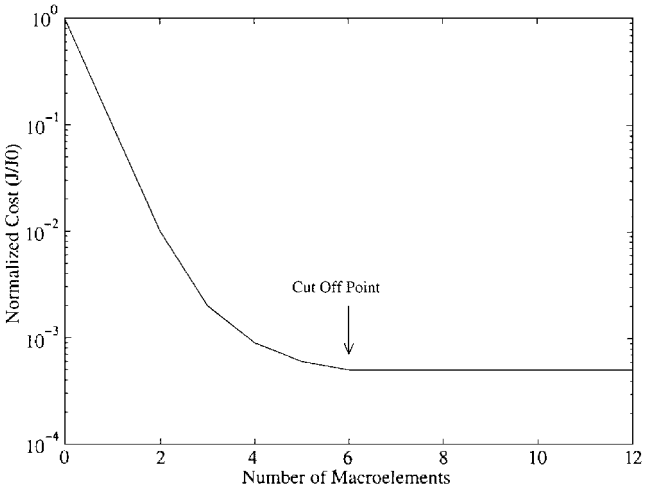

Fig. 3 Example of the reduction of macroelements using the weighted least squares cost.

E. Accuracy of Uncertainty Model

Although the development of a practical algorithm for uncertainty modeling is fairly complete, there were a number of assumptions that should be addressed. First, the assumption that the macroelements in Eq. (11) accurately represent the errors of the system is important. Reference 18 gives a summary of how each of these uncertainties affect the localization process. Examining Table 1, those uncertainties termed difficult to capture, such as modeling method, cannot be accurately represented by a physical mass and stiffness uncertainty, as in Eq. (11). To successfully identify and localize uncertainties, the following steps must be taken to reduce the effects of these types of uncertainties.

1) Refine the finite element mesh to prevent discretization and joint/attachment errors.

2) Understand the physics of the system such that correct element types are used.

3) Completely model boundary conditions and actuator and sensor dynamics.

4) Understand all coupling effects and their impact on the FEM.

5) Understand all nonlinear effects, including modeling highly nonlinear components.

Although this list is usually quite difficult to complete, these uncertainties need to be small for the process to work well. If these precautions cannot be met, the only other recourse is to increase the scaling on the bound factors in Eqs. (25) and (26), thus creating a more conservative uncertainty model.

For the other uncertainties, termed easy to capture, only the physical parameters can clearly be represented using physical macroelements. Most coupling dynamics are parameterized in the identification process and are not localized. One exception to this is gravity effects, for which subelement-based macroelements can be developed. It is assumed that testing uncertainties sensor and process noises are small or could be made small within the parameter estimation procedure using methods such as averaging. The effects of weak nonlinearities unfortunately are difficult to quantify and evaluate. Therefore, it is assumed that these can be modeled within the parameter bounds.

A second important assumption that is made is the model is an accurate description of the hardware, as given by Eq. (9). To evaluate this, a second-order term of the eigenvalue perturbation expansion is considered. The method is assumed to be valid when the second-order term is less than 20% of the first-order terms. For the eigenvalue error, this is written as

$$\frac{(\Delta\lambda_i)^2}{\lambda_i} > 0.2 \cdot \Delta\lambda_i \qquad \text{or} \qquad \Delta f_i < 0.1 \cdot f_i \tag{30}$$

Although the mean errors in frequencies are usually larger than 10%, these can be reduced by using the mean errors in a traditional iterative updating technique in order to ensure Eq. (30) is met and the system can, indeed, be represented using a first-order expansion. The parameter bounds, however, cannot be updated. Therefore, the parameter bounds should be within those set in Eq. (30).

V. Small-Order Example

Figure 4 shows a small-order example used to analyze the techniques developed and to add insight to the uncertainty localization and projection methods. It is a planar system with four tubular cross-sectioned struts and three concentrated mass/inertia collars. There are eight beam elements and eight nodal points with 3 degrees of freedom for each (vertical, horizontal, and rotational) giving 24 degrees of freedom. The mass and stiffness matrices for these elements are standard displacement-based two-dimensional beam elements. The mass matrix is chosen to be in consistent form. The L shape couples the vertical and horizontal displacements.

Table 2 Summary of small-order example, uncertainties simulated in the form of a normal variable with mean and standard deviation errors $[(\cdot) = N(\overline{\Delta(\cdot)}), \sigma_{\Delta(\cdot)}]$

Uncertainties, %	Measurements	Frequencies, Hz: Nominal (cantilevered)	Frequencies, Hz: Modified (free)
$E_2 = N(5, 2)$	First four frequencies	3.1	0.0
$L_4 = N(-5, 0)$	u_1, u_3, u_5, u_7	18.2	0.0
$r_6 = N(-5, 2)$		43.1	0.0
$m_{67} = N(3, 0)$		72.8	22.3
		97.3	44.8
		120.2	83.3
		131.2	110.3

Table 3 Localization results of the mean errors in mass and stiffness matrices of small-order example, % error

Stiffness			Mass		
Entry	Actual	Local	Entry	Actual	Local
1 · 1	2.4	2.2	7 · 7	−2.6	−2.7
2 · 2	2.4	2.2	8 · 8	−2.6	−2.7
3 · 3	2.4	2.2	9 · 9	−7.7	−8.0
8 · 8	7.7	7.8	10 · 10	−0.2	−0.2
9 · 9	2.6	2.6	11 · 11	−0.2	−0.2
11 · 11	7.7	7.9	12 · 12	−0.1	−0.1
13 · 13	−2.6	−2.4	13 · 13	−2.6	0.0
14 · 14	−7.7	−7.7	16 · 16	2.6	2.6
16 · 16	−4.9	−4.6	17 · 17	2.5	2.6
18 · 18	−7.7	−7.7	18 · 18	2.9	2.8
Average residual		0.1	Average residual		0.1

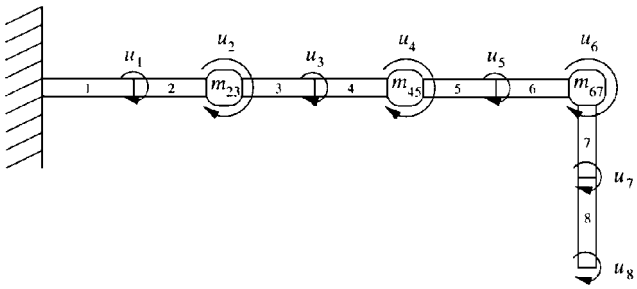

Fig. 4 Small-order example: cantilevered L beam.

The nominal system is the cantilevered configuration, whereas the modified system is a change in operational environment to the free-free configuration, shifting frequencies by 20–50%. (Note the damping is proportional and 1% for all modes.) The free-free configuration has nine nodal points and 27 degrees of freedom. Table 2 gives a summary of the simulated problem, including the system measurements and uncertainties (both mean and varying) that are introduced. The simulation entails sampling the stochastic uncertainties and introducing them into the nominal and modified models to create a set of cases for the true systems. The mean and variance of both the mean error and variance uncertainties in both the nominal and modified systems were calculated. For this simulation, 10 cases were run.

A two-step localization procedure was used. Table 3 shows the actual and localized results for a few entries in the mass and stiffness matrices. In most cases, the physical errors are predicted quite well. An overall mass mean error of 2.35% is reduced to 0.1% (for those entries in error), and a stiffness mean error of 3.98% is reduced to 0.1%. The localized results of the variance uncertainties showed comparable results. Because the physical mass and stiffness uncertainties are localized quite well, the prediction of the modified uncertainty model (and, therefore, the projection method) is expected to be quite accurate. Figure 5 shows the results of the prediction of the modified FEM frequencies, using 10 simulated cases. Note that each point is normalized by the corresponding modified FEM frequency. Each simulated case is within the predictions, indicating an accurate prediction of the modified uncertainty model, even though only four modes and mode shapes were measured.

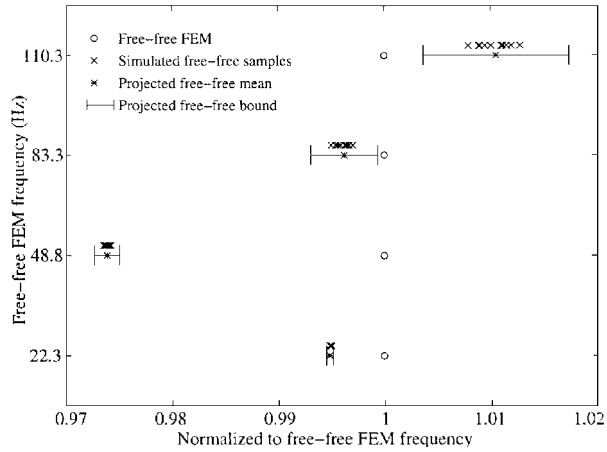

Fig. 5 Frequency prediction results for the small-order example.

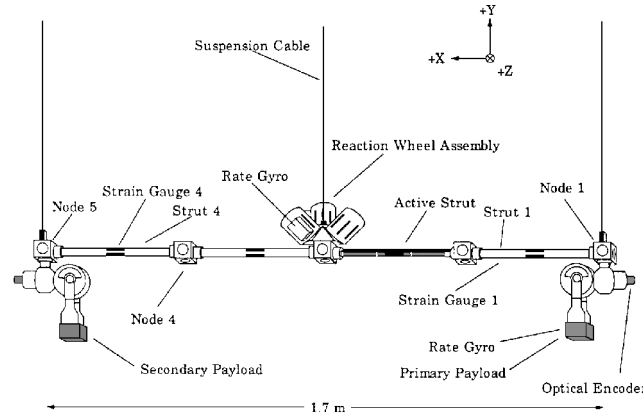

a) MACE Configuration I 1-*g*

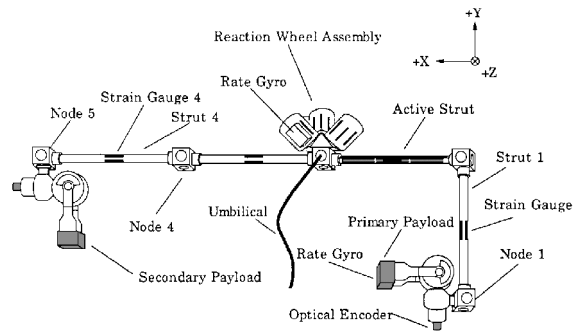

b) MACE Configuration II 0-*g*

Fig. 6 MACE test article.

VI. Experimental Verification

The Middeck Active Control Experiment (MACE) was designed to be a reusable dynamics and control laboratory for the investigation of issues associated with a change in operational environment of a flexible spacecraft from ground- to space-based operations. An extensive set of modeling and control experiments were performed on the test article during 14 days of on-orbit operations while on STS-67 in March 1995 (Ref. 19). Note that a matrix method was used to develop the 0-*g* uncertainty model for the MACE flight,[20] whereas the sensitivity method was developed after the flight to improve on inadequacies in the matrix method, i.e., the use of partial information.

Figure 6 shows two configurations of the MACE test article that were utilized. The first is MACE Configuration I, which contains a straight bus (as shown in 1-*g* in Fig. 6a). Figure 6b shows Configuration II, which contains an L bus (as shown in 0-*g* in Fig. 6b). Note that Configuration II was not tested on the ground. Because there were multiple configurations of the MACE test article flown on STS-67, the prediction of uncertainty models can be tested on

Table 4 Summary of model and data parameters of the two experimental MACE examples

Property	Configuration I 1-g	Configuration I 0-g	Configuration II 0-g
Degrees of freedom (DOF), $n_{(\cdot)}$	678	480	480
FEM modes	375	280	280
Measured DOF, $r_{(\cdot)}$	17(9 XY, 8 Z)	17(9 XY, 8 Z)	17(9 XY, 8 Z)
Measured frequencies, $\tilde{n}_{(\cdot)}$	24(14 XY, 10 Z)	24(14 XY, 10 Z)	24(14 XY, 10 Z)
Data sets	16	12	4
Stiffness elements	99	69	69
Mass elements	59	32	32
Concentrated spring elements	9	0	0
Concentrated mass elements	39	33	33

two distinct examples for experimental verification. The first example is MACE Configuration I in 1-g to Configuration I in 0-g, thus testing a change in gravity environment. The second example is MACE Configuration I in 0-g to Configuration II in 0-g, thus testing a change in configuration.

A. MACE Configuration I 1-g to 0-g

The first example is using MACE Configuration I in 1-g to predict the uncertainties for MACE Configuration I in 0-g. This example is motivated by those spacecraft that can only be tested on the ground, prior to flight. For MACE, this example was the basis for most controllers developed prior to flight. Because of the removal of gravity and suspension degrees of freedom, this prediction is quite a challenging task.

The FEM for the nominal system (Configuration I in 1-g) contains $n_N = 678$ degrees of freedom, and 375 modes are retained. There are 16 data sets available for identification, producing $r_N = 17$ measured degrees of freedom (9 in XY axes + 8 in Z axis) and $\tilde{n}_N = 24$ measured frequencies (14 in XY axes + 10 in Z axis). This gives 230 measured modal uncertainties in the MACE 1-g uncertainty model (140 in XY axes + 90 in Z axis). The FEM for the modified system (Configuration I in 0-g) contains $n_M = 480$ degrees of freedom, while 280 modes are retained. There are 12 data sets available for identification, producing $r_N = 17$ measured degrees of freedom (9 in XY axes + 8 in Z axis) and $\tilde{n}_N = 24$ measured frequencies (14 in XY axes + 10 in Z axis). A summary of the specific parameters of this example is given in Table 4.

Because there are 230 measured nominal uncertainties and 206 elements in the nominal 1-g FEM, only two steps of uncertainty localization are required: at the element and at the subelement levels. Two different forms of subelement-based macroelements were used for this example, based on beam parameters and gravity parameters. Because most of the beam elements contain tubular cross sections, there are six physical parameters that could be used to developing macroelements: modulus of elasticity ΔE, density $\Delta\rho$, length ΔL, radius Δr, thickness Δt, and Poisson's ratio $\Delta\nu$. For this example, only ΔE, $\Delta\rho$, and ΔL are used as macroelements, giving two independent mass and two independent stiffness subelements. The other three uncertainties can be approximated using combinations of these macroelements, assuming that the primary modes of interest are bending. The second type of subelement-based macroelement is a function of the gravity modeling.[17] The primary gravity effects are gravity stiffening and initial sag in the Lexan beam elements, gravity stiffening in the gimbals, and tensioning in the suspensions cables. Because these effects are modeled as a superposition to the stiffness element, macroelements can be developed that are also at the subelement level.

Step 2 (localization of the nominal uncertainties) revealed that most uncertainties lay within the physical and gravity parameters of the Lexan beam elements. Surprisingly, there were few localized uncertainties in the suspension cables, where very large gravity effects exist in the tensioning of the cables. This may be a result of the lack of measured suspension modes and degrees of freedom. Step 3 (mapping) included mapping of test article degrees of freedom but not suspension degrees of freedom into 0-g, thus giving

$$T_{MN} = [I_{480} \quad 0_{480\cdot 198}] \tag{31}$$

In addition, the gravity macroelements were not mapped into 0-g.

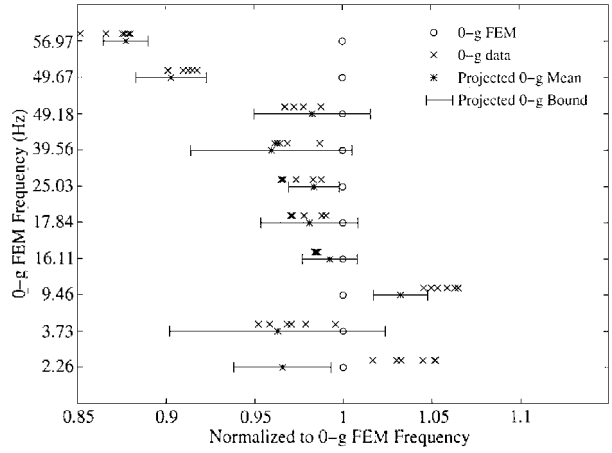

Fig. 7 Results of MACE 1-g to 0-g frequency uncertainty model prediction.

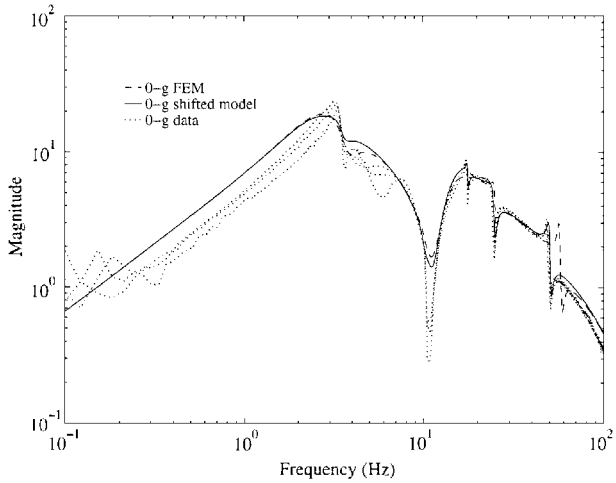

Fig. 8 MACE 0-g FEM, 0-g FEM shifted by predicted mean errors, and three sets of data.

Figure 7 shows the predicted and actual results for the modified 0-g frequencies. The prediction of mean errors and bounds is excellent for all but the 2.26- and 9.46-Hz modes. In addition, there are one or two data points outside the predicted bounds. For each of these data points, the parameter estimate had not converged in the identification process because the parameter is nearly unobservable or uncontrollable. With more time-domain data, these estimates would be within the predicted ranges as well.

To show the results of the mode shape predictions, Fig. 8 shows transfer functions from primary X gimbal to primary X rate gyro using: the 0-g FEM, the 0-g FEM shifted by the predicted mean errors of the modified uncertainty model, and three 0-g data sets. Although similar, there are two important regions of improvement of the shifted model. First, at high frequency, the 56.97-Hz mode has been predicted correctly, whereas there is a 15% error in the FEM. Second, the prediction of the 17.84-Hz mode of the shifted model

Table 5 Variations between 1-*g* and 0-*g* and Configuration I and Configuration II cases as predicted by the FEM and as measured in the data; large deviations between FEM and data indicate large modeling errors

1-*g* frequency, Hz	1-*g* to 0-*g*, %		Configuration I to Configuration II, %	
	FEM	Data	FEM	Data
2.24	−1.1	−7.8	−4.6	−8.0
4.60	18.9	17.7	−53.0	−43.4
9.79	3.3	2.4	13.6	11.1
16.19	0.4	4.1	−18.3	−17.8
17.82	−0.1	1.7	0.5	1.3
24.89	−0.5	2.9	−4.5	−3.7
39.41	−0.3	0.0	26.9	19.7
48.84	−0.6	4.2	8.8	13.1
49.01	−1.3	−0.9	28.6	25.4
56.16	−1.4	7.8	0.5	12.4

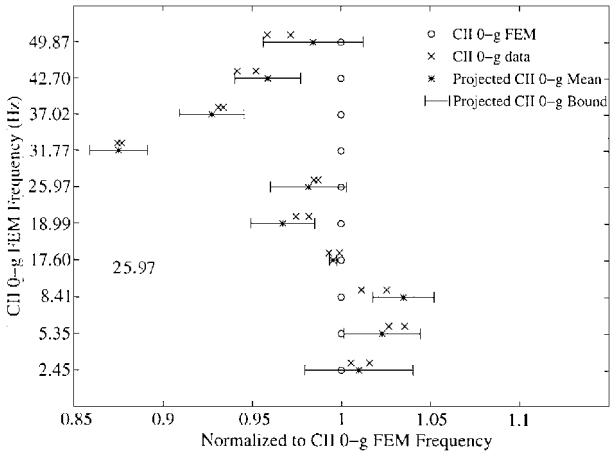

Fig. 9 Results of the MACE Configuration I to Configuration II frequency uncertainty model prediction.

has correctly changed the sign of the FEM residue, thus matching the actual residue of the data sets.

Although the prediction of the MACE 0-*g* uncertainty worked well, the 2.26- and 9.46-Hz frequencies are troublesome. The primary reason for these discrepancies are that these two modes are highly coupled with gravity. Although one objective of this process is to differentiate between hardware and gravity modeling errors, in reality this is quite difficult to do. Gravity effects can usually only be accurately modeled and updated by using a large number and different types of sensors.[17] This is because gravity effects are modeled by a superposing addition to the stiffness matrix. For MACE, only 17 of the 678 degrees of freedom were measured, and many of these sensors were on large, stiff members of the system (gimbal, reaction wheels) rather than on the flexible parts of the system (struts). Table 5 shows a summary of the shift in frequency from 1-*g* to 0-*g* as predicted by the FEM and as measured in the data. Numbers that are closed indicate a high degree of accuracy in the modeled gravity effects. For some modes, such as 4.60 Hz, the FEM predicts the changes quite well. For other modes, however, such as 17.82, 24.89, and 56.16 Hz, the predicted change is incorrect in sign and magnitude. In subsequent simulations after the MACE flight, the addition of more sensors improved the gravity modeling and improved the predicted estimates of the errors of these modes.

B. MACE 0-*g* Configuration I to Configuration II

The second example is using MACE Configuration I in 0-*g* to predict the uncertainties for MACE Configuration II in 0-*g*. This example is motivated by those systems that must be tested in a configuration that is different than its eventual use. This example is much simpler than the preceding example because there are no modeled suspension and gravity effects.

The nominal system (Configuration I in 0-*g*) has available 12 data sets and 134 measured modal uncertainties for the nominal uncertainty model (80 in XY axes + 54 in Z axis). For comparison, the modified system (Configuration II in 0-*g*) has available only 4 data sets. Configuration II was developed by simply rotating those degrees of freedom in the bottom part of the L configuration (Fig. 6b). Therefore, the mapping of degrees of freedom is given by

$$T_{MN} = \begin{bmatrix} I_{360} & 0_{360\cdot 120} \\ 0_{120\cdot 360} & T_{120} \end{bmatrix} \tag{32}$$

where T_{120} is a rotation matrix.

Figure 9 shows the predicted and actual results for the modified Configuration II frequencies. All but two points (8.41 and 17.60 Hz) lay within the predicted uncertainty model. In each of these cases, the parameter estimate again had not converged. Table 5 shows a summary of the shift in frequency from Configuration I and Configuration II as predicted by the FEM and as measured by the data. Although the magnitude is not always correct, the general trends are very good. This shows that the overall modeling of the MACE test article is very good, thus improving the accuracy of predicting the remaining small uncertainties. In addition, this example reiterates that the 1-*g* to 0-*g* MACE example is quite difficult because of the gravity modeling and could be improved with more system measurements.

VII. Conclusions

A set of methods to identify structural uncertainties between a model and hardware in a nominal environment and to predict an uncertainty model in a modified environment have been developed. A summary of the many uncertainties that may exist in a structural system is given. The sensitivity method, because of its ability to handle incomplete measured uncertainties, is used to localize uncertainties to specific degrees of freedom. A practical algorithm is presented, which limits the number of mass and stiffness uncertainties and uses a layered approach to localize uncertainties in groups of elements, then in elements, then in subelements. A small-order sample problem showed the method worked well in predicting and identifying both mean and variance uncertainties in the mass and stiffness matrices using a subset of measured modes and degrees of freedom.

Two examples of the MACE system were used to experimentally verify the prediction of a modified uncertainty model. The MACE 1-*g* to 0-*g* example performed quite well, but with small residual errors, which were a result of a lack of sensors for gravity modeling update. The MACE 0-*g* Configuration I to Configuration II prediction results were very accurate, primarily because the MACE system was well modeled, and there were no gravity effects in the problem. Overall, the development and prediction of structural uncertainty models is mature enough to use for applications such as model prediction, closed-loop control, and structural redesign.

Acknowledgments

This work was supported by the NASA IN-STEP Program and NASA Langley Research Center CSI Office with Gregory Stover and Jerry Newsom as Contract Monitors, under Contracts NAS1-18690 and NAS1-19622.

References

[1]Caesar, B., "Updating System Matrices Using Model Test Data," *Proceedings, International Modal Analysis Conference*, Union College, Schenectady, NY, 1987, pp. 453–459.

[2]Link, M., "Identification and Correction of Errors in Analytical Models Using Test Data—Theoretical and Practical Bounds," *Proceedings, International Modal Analysis Conference*, Society for Experimental Mechanics, Bethel, CT, 1990, pp. 570–578.

[3]Maia, N., Reynier, M., and Ladeveze, P., "Error Localization for Updating Finite Element Models Using Frequency Response Functions," *Proceedings, International Modal Analysis Conference*, Society for Experimental Mechanics, Bethel, CT, 1994, pp. 1299–1308.

[4]Sidhu, J., and Ewins, D. J., "Correlation of Finite Element and Modal Test Studies of a Practical Structure," *Proceedings, International Modal Analysis Conference*, Union College, Schenectady, NY, 1984, pp. 756–762.

[5]Gysin, H., "Critical Application of the Error Matrix Method for Localisation of Finite Element Modeling Inaccuracies," *Proceedings, International Modal Analysis Conference*, Union College, Schenectady, NY, 1986, pp. 1339–1351.

[6]Lallement, G., "Indirect Identification Methods I: Adjustment of Mathematical Models by the Results of Vibrating Tests: Using Eigensolutions," *Identification of Vibrating Structures*, edited by H. G. Natke, Springer–Verlag, New York, 1982, pp. 179–194.

[7]Piranda, J., Lallement, G., and Cogan, S., "Parametric Correction of Finite Element Models by Minimization of an Output Residual: Improvement of the Sensitivity Method," *Proceedings, International Modal Analysis Conference*, Society for Experimental Mechanics, Bethel, CT, 1991, pp. 363–368.

[8]Fissette, E., Stavrinidis, C., and Ibrahim, S., "Error Location and Updating of Analytical Dynamic Models Using a Force Balance Method," *Proceedings, International Modal Analysis Conference*, Society for Experimental Mechanics, Bethel, CT, 1989, pp. 1063–1070.

[9]Gordis, J. H., "An Exact Formulation for Structural Dynamic Model Error Localization," *Proceedings, International Modal Analysis Conference*, Society for Experimental Mechanics, Bethel, CT, 1993, pp. 159–167.

[10]He, J., "Sensitivity Analysis and Error Matrix Method Using Measured Frequency Resonse Function (FRF) Data," *Proceedings, International Modal Analysis Conference*, Society for Experimental Mechanics, Bethel, CT, 1993, pp. 1079–1082.

[11]Crawley, E. F., Barlow, M. S., van Schoor, M. C., Masters, B. P., and Bicos, A. S., "Measurement of the Modal Parameters of a Space Structure in Zero Gravity," *Journal of Guidance, Control, and Dynamics*, Vol. 18, No. 3, 1995, pp. 385–392.

[12]Collins, J. D., Hart, G. C., Hasselman, T. K., and Kennedy, B., "Statistical Identification of Structures," *AIAA Journal*, Vol. 12, No. 2, 1972, pp. 185–190.

[13]Hasselman, T. K., Chrostowski, J. D., and Ross, T. J., "Interval Prediction in Structural Dynamic Analysis," *Proceedings of the AIAA Structures, Structural Dynamics, and Materials Conference* (Dallas, TX), AIAA, Washington, DC, 1992, pp. 1272–1284.

[14]Hasselman, T. K., Chrostowski, J. D., and Ross, T. J., "Propagation of Modeling Uncertainty Through Structural Dynamic Models," *Proceedings of the AIAA Structures, Structural Dynamics, and Materials Conference* (Hilton Head, SC), AIAA, Washington, DC, 1994, pp. 72–83.

[15]Campbell, M. E., "Identification and Parameter Estimation for Control Design," *Proceedings, IFAC 13th World Congress* (San Francisco, CA), Vol. 1, Elsevier Science, Oxford, England, UK, 1996, pp. 209–214.

[16]Gysin, H., "Comparison of Expansion Methods for FE Modeling Error Localization," *Proceedings, International Modal Analysis Conference*, Society for Experimental Mechanics, Bethel, CT, 1990, pp. 195–204.

[17]Rey, D. A., Crawley, E. F., Alexander, H., Glaese, R., and Gaudenzi, P., "Gravity and Suspension Effects on the Dynamics of Controlled Structures," *Proceedings of the AIAA Structures, Structural Dynamics, and Materials Conference* (La Jolla, CA), AIAA Washington, DC, 1993, pp. 3156–3171.

[18]Campbell, M. E., "Uncertainty Effect in Model-Data Correlation," *Proceedings of the 38th Structures, Structural Dynamics, and Materials Conference* (Kissimmee, FL), AIAA, Reston, VA, 1997.

[19]Miller, D. W., How, J. P., Liu, K., Campbell, M. E., Glaese, R. M., Grocott, S. C. O., and Tuttle, T. D., "Flight Results from the Middeck Active Control Experiment (MACE)," Space Engineering Research Center, Rept. 7-96, Massachusetts Inst. of Technology, Cambridge, MA, 1996; also *AIAA Journal* (submitted for publication).

[20]Campbell, M. E., Grocott, S. C. O., How, J. P., Miller, D. W., and Crawley, E. F., "Verification Procedure for On-Orbit Controllers for the Middeck Active Control Experiment," *Proceedings, 1995 American Control Conference* (Seattle, WA), Inst. of Electrical and Electronics Engineers, Piscataway, NJ, 1995, pp. 3600–3605.